International Dairy Journal 154 (2024) 105941

Contents lists available at ScienceDirect

International Dairy Journal

journal homepage: www.elsevier.com/locate/idairyj

Effect of acetic acid solutions on regenerated fibers from rennet-treated casein micelles

Novin Darvishsefat , Md Asaduzzaman , Calvin Hohn , Ronald Gebhardt *

Chair of Soft Matter Process Engineering (AVT.SMP), RWTH Aachen University, 52062 Aachen, Germany

ARTICLE INFO

Article history:
Received 7 December 2023
Received in revised form
11 March 2024
Accepted 14 March 2024
Available online 24 March 2024

ABSTRACT

Fibers made from rennet casein micelles promise a wide range of new applications in food-grade products. Understanding the influence of environmental conditions such as pH on the water binding and swelling properties is a crucial factor for embedding them in hydrated matrices in the future. The expansion of the fibers in dilute acetic acids always takes place in two steps, as previously observed in citric acid. Model analyses showed that the rates of the swelling steps decreased with increasing acetic acid strength. In contrast, the simulated plateau values of both swelling steps increased. Differences to swelling in citric acid are discussed for the second swelling step on the basis of the pH value of the swelling media, while different calcium affinities are assumed for the first swelling step.

1. Introduction

The processing of casein fibers from enzymatically treated casein micelles does not require drastic pH changes and additives compared to conventional methods (Sudha, Thanikaivelan, Ashokkumar, & Chandrasekaran, 2011; Thill, Schmidt, Wöll, & Gebhardt, 2021; Tomasula et al., 2016; Yang & Reddy, 2012). They can therefore be functionalized for food-grade applications, e.g. as a matrix for the encapsulation and controlled release of e.g. bioactive substances. Aggregated casein structures are currently being developed as carriers for bioactive substances such as polyphenols and vitamins in food, antibacterial agents in animal feed or drugs in cancer therapy (Bar-Zeev, Kelmansky, Assaraf, & Livney, 2018; Chen et al., 2020; Sadiq, Gill, & Chandrapala, 2021). Caseins are natural nanocarriers for highly insoluble calcium phosphate, small bioactive molecules or larger macromolecules due to their supramolecular aggregated structure in milk (Dalgleish, 2011). These so-called casein micelles, which we use as the starting material for the fibers, consist of four different caseins in cow's milk, which have direct contact via hydrophobic, van der Waals and hydrogen bonds or can also be bridged via their phosphoseryl residues by calcium, calcium phosphate or micellar calcium phosphate (Hindmarsh & Watkinson, 2017). An approximately 10 nm thick polymer brush formed by κ-casein on the surface provides colloidal stability through steric repulsion (De Kruif & Zhulina, 1996). If the Phe105-Met106 bond of the κ-casein is specifically cleaved by the protease chymosin, para-casein micelles are formed, which are colloidally unstable and aggregate under normal conditions (Dalgleish & Corredig, 2012; Horne & Lucey, 2017). However, the coagulation process can be prevented at low temperatures, which opens up a number of new possibilities to produce functionalized casein-based gel structures (Heidebach, Först, & Kulozik, 2009; Warncke, Keienburg, & Kulozik, 2021) or to investigate the aggregation process decoupled from the enzymatic destabilization step (Thill, Schmidt, Wöll, & Gebhardt, 2020). For fiber production, the cold-stored para-casein micelles are extruded through a capillary into a warm coagulation bath. While the new process promises many improvements in terms of sustainability goals, there are challenging research questions regarding water-binding properties and stability.

After drying, post-treatment steps such as covalent cross-linking can be carried out before the swelling behavior and mechanical properties are investigated. The fibers expand in aqueous solutions at neutral pH or in 1 N HCl solution to an equilibrium swelling value, while dissociation occurs in 1 N NaOH after swelling (Thill, Schmidt, Jana, Wöll, & Gebhardt, 2022; Thill et al., 2021). TGase cross-linking stopped the decomposition in NaOH. Interestingly, as a result of the enzymatic post-treatment, the young moduli of the dried fibers also decreased as was also observed for fibers produced with the plasticizer glycerol (Thill & Gebhardt, 2022). Recently, we have shown that the fibers also swell strongly in organic acids such as citric acid or acetic acid (Gebhardt & Darvishsefat, 2023). Their effect on water binding is of particular interest as they are added as cross-linking and coagulation agents

* Corresponding author.
E-mail address: ronald.gebhardt@avt.rwth-aachen.de (R. Gebhardt).

https://doi.org/10.1016/j.idairyj.2024.105941

in traditional casein fiber production (Yang & Reddy, 2012) and both acidulants showed highest protein recovery in pre-cheeses (Seth & Bajwa, 2015). If the pH drops below 5.3, all the micellar calcium phosphate dissolves in the casein micelles (Dalgleish & Law, 1988), with all the inorganic phosphate and, from pH 3.5, also all the calcium being in solution (Gaucheron, 2005). However, destabilization can also occur via a chelating agent such as citrate, which causes increased swelling even at neutral pH conditions due to a more negative charge state of the casein (Asaduzzaman, Pütz, & Gebhardt, 2022). Compared to acetic acid, pre-acidification of milk with citric acid reduced the calcium in the resulting rennet gel more (Metzger, Barbano, Rudan, & Kindstedt, 2000). The acid-induced gel formation of casein micelles with partially hydrolyzed κ-casein can be investigated with dynamic rheological experiments (Gastaldi et al., 2003). A sigmoidal increase in storage modulus was observed in the course of rennet-induced skimmed milk gel formation (Zoon, 1988) and after acidification with glucono-δ-lactone for acidified milk gels (Horne, 1999).

In this study, we investigate the influence of acetic acid on fiber swelling. For this purpose, we use solutions <5.7 vol.%, more precisely 0.125, 0.5 and 1 M acetic acid to minimize the influence on the water activity and to have a comparison of the results with previous findings in citric acid. Since acetic acid is the weaker acid, the pH of the swelling media shifts to higher pH values. In addition, acetic acid has a simpler molecular structure compared to citrate and cannot act as a chelating agent for calcium. For the analysis, we use the sequential swelling model, which has already been used for the two-step kinetics in HCl and citric acid (Gebhardt & Darvishsefat, 2023; Thill et al., 2022) and discuss the effects of the acetic acid solutions on both swelling steps comparatively. The results of the study are relevant for the future use of the fibers as encapsulation material for bioactive food components or for the immobilization of enzymes under acidic pH conditions, especially in acetic acid media.

2. Material and methods

Fig. 1 summarizes the individual process steps for sample preparation and analysis of fiber swelling. The sample preparation from raw milk to dried fiber takes about 48 h, with the renneting of the micellar casein sample in the cold for 24 h being the longest process step. While the swelling of the fibers takes a few minutes, the digitization of the data takes several hours and the numerical analysis of the swelling data takes days. The individual process steps are described in detail below.

2.1. Raw material

Casein micelles were obtained using fresh whole milk from a local farmer (Soerser Milchkännchen, Aachen, Germany). After fat separation at 3000×RCF for 20 min in a centrifuge (Hettich Universal 320 R centrifuge), the milk was then centrifuged at 70 000×RCF for 60 min in an OptimaXP-80 ultracentrifuge (Beckman Coulter GmbH, Krefeld, Germany) to separate the casein micelles from the whey proteins. The casein pellet was resuspended in simulated milk ultrafiltrate (SMUF) by stirring at 37 °C for 2 h. The SMUF buffer was prepared according to Dumpler, Kieferle, Wohlschläger, & Kulozik (2017), and contained 10 different mineral salts. To prevent microbial growth, 0.05% (w/w) sodium azide (99%, Carl Roth, Karlsruhe, Germany) was added to the SMUF buffer. The casein micelle concentration was later measured with a Sartorius moisture balance (MA37-1) and finally the casein concentration was adjusted to 5% (w/w) by dilution with SMUF.

2.2. Chymosin treatment in the cold

Casein micelles were incubated with 100 IMCU L-1 chymosin (Chymosin CHY-MAX M, Chr. Hansen A/S, Hoersholm, Denmark) at 5 °C for 24 h in a refrigerator to obtain a stable para-casein micelle solution.

2.3. Fiber production

The renneted casein solution was extruded into a hot, calcium chloride-rich coagulation bath (T = 60 °C, 100 mM calcium chloride (Carl Roth, Karlsruhe, Germany)) using a syringe pump (flow rate 0.4 mL min^{-1}), with the dosing needle having an inner diameter of 0.8 mm. The obtained fiber pieces were removed and placed on a rack to ensure that they were dried in air without direct contact with the surface, resulting in a cylindrical shape. Dried fiber pieces with a length of approximately 3 cm were used for the swelling test under the microscope.

2.4. Swelling experiments

After the casein fiber pieces were completely dried, they were fixed on a transparent Petri dish and placed on an inverted microscope with the light source at the top and the camera at the bottom (Nikon eclipse TE300, Tokyo, Japan). Different acidic solutions with a molarity of 0.125 M, 0.5 M and 1 M were prepared from 100% acetic acid (Carl Roth, Karlsruhe, Germany) and poured onto the fibers, ensuring that they were completely immersed. The video of the swelling process was recorded with a microscope-mounted camera (AMscope Camera, USA). Finally, screenshots of the videos were taken for each swelling time.

2.5. Evaluation of the images and swelling curves

For each acetic acid solution, the progress of swelling was observed on three different fiber pieces. For this purpose, the fiber thickness was determined for each fiber at three distinct points in time. After averaging, the increase in fiber thickness for all individual fibers was calculated from the fiber thickness at time t, d_t and the initial fiber thickness, d_0, as follows:

$$\textit{Width increase}\ (\%) = \left(\frac{\langle d_t \rangle}{\langle d_0 \rangle} - 1\right) \cdot 100 \tag{1}$$

The increase in width was then plotted as a function of time and analyzed.

2.6. Dynamic modelling of the swelling process

A second-order swelling kinetics (Schott, 1992):

$$S = \frac{k_S \cdot S_\infty^2 \cdot t}{1 + k_S \cdot S_\infty^2 \cdot t} \tag{2}$$

describes the swelling process for micellar casein fibers in water under neutral pH conditions with S the solvent uptake at time t, S_∞ the swelling value reached at time $t \to \infty$ and k_S, the specific swelling rate (Thill et al., 2022).

Based on the swelling rate

$$\frac{dS}{dt} = k_S \cdot (S_\infty - S)^2 \tag{3}$$

with $(S_\infty - S)^2$ the remaining swelling capacity, an extended model for analyzing two-step swelling kinetics in HCl and citric acid

solutions was developed (Gebhardt & Darvishsefat, 2023; Thill et al., 2022).

$$\frac{dS}{dt} = w_1 \cdot k_1 \cdot (S_{1,\infty} - S)^2 +/_- w_2 \cdot k_2 \cdot (S_{2,\infty} - S)^2 \quad (4)$$

Specific swelling rates and remaining swelling capacities are considered for both steps via the indices 1 and 2. The transition between the two swelling steps is described via the time-dependent ratios w_1 and w_2

$$w_1 = \left(\frac{1}{1+g(t)}\right), w_2 = \left(\frac{g(t)}{1+g(t)}\right) \quad (5)$$

using a simple exponential function with a characteristic time t' and rate k_t

$$g(t) = e^{(t-t')\cdot k_t} \quad (6)$$

In order to calculate the proportions of swollen structure, the swelling rates of the individual swelling steps were integrated over the past swelling time.

$$S_{i=1,2} = \int_{t=0}^{t} w_i \cdot \frac{dS_i}{dt} dt \quad (7)$$

3. Results and discussion

The process described in Fig. 1 can be used to prepare fibers up to 10 cm long, which can be bent in the dry state without breaking (Fig. 2, left). If the dried fibers are brought into contact with acetic acid solutions, they continue to swell until the contrast between the fiber edge and the solvent disappears after approx. 200 s. However, there is no evidence of dissolution of the fiber, such as in 1 M NaOH by splitting the edge region into micrometer-sized fragments (Thill et al., 2021). It can already be observed under the microscope that swelling occurs in two stages in 0.125 M acetic acid, while more continuous fiber growth takes place in 1 M acetic acid (Fig. 2, right). Under certain acidic conditions (e.g. after 60 s in 0.5 M acetic acid), fiber bending occurs in addition to swelling, which is currently being investigated. For a more detailed and comparative analysis, the fiber thicknesses during swelling were determined from the microscopic images of the video sequences. The increase in fiber thickness was then calculated using Equation (1) and plotted as a function of time.

Three fibers from different fiber preparations were swollen per acetic acid concentration. Fig. 3 shows a representative swelling curve in 0.125 M, 0.5 M and 1 M acetic acid, whereby the values were obtained by averaging the thickness increase at three points of a fiber. As already reported for the swelling medium citric acid (Gebhardt & Darvishsefat, 2023), the fibers also swell in acetic acid in a two-step process. Both steps are particularly evident in

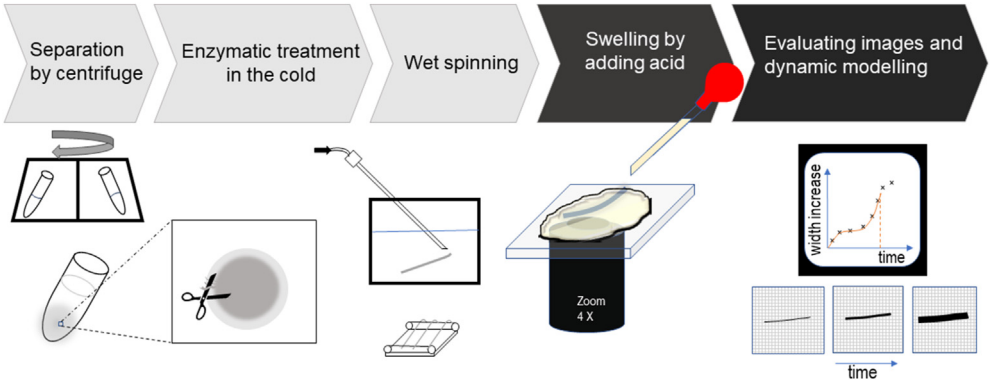

Fig. 1. Flow diagram of the sequential process steps for the sample preparation of casein fibers and for the analysis of fiber swelling.

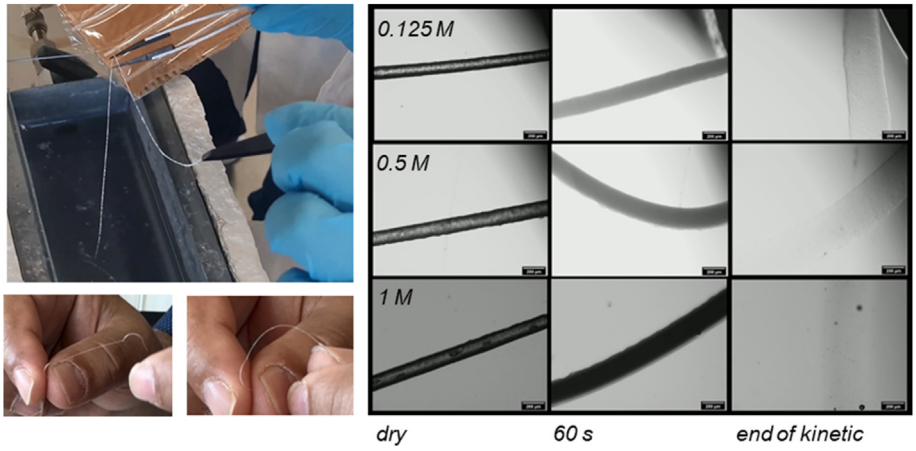

Fig. 2. Left) Fiber harvesting from the coagulation bath and flexibility test after drying; right) selected microscopic images (scale bar: 200 μm) from the swelling sequence in acetic acid solutions with different concentrations.

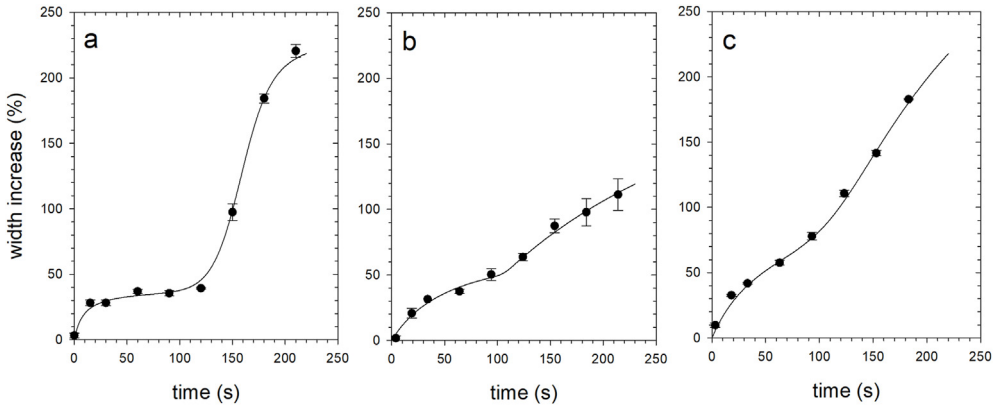

Fig. 3. Representative swelling curve of regenerated casein fibers in a) 0.125 M, b) 0.5 M and c) 1 M acetic acid. The error bars correspond to the standard deviation of the values measured at three different points on a fiber. The solid lines correspond to simulated swelling values with the swelling model (Equation (4)).

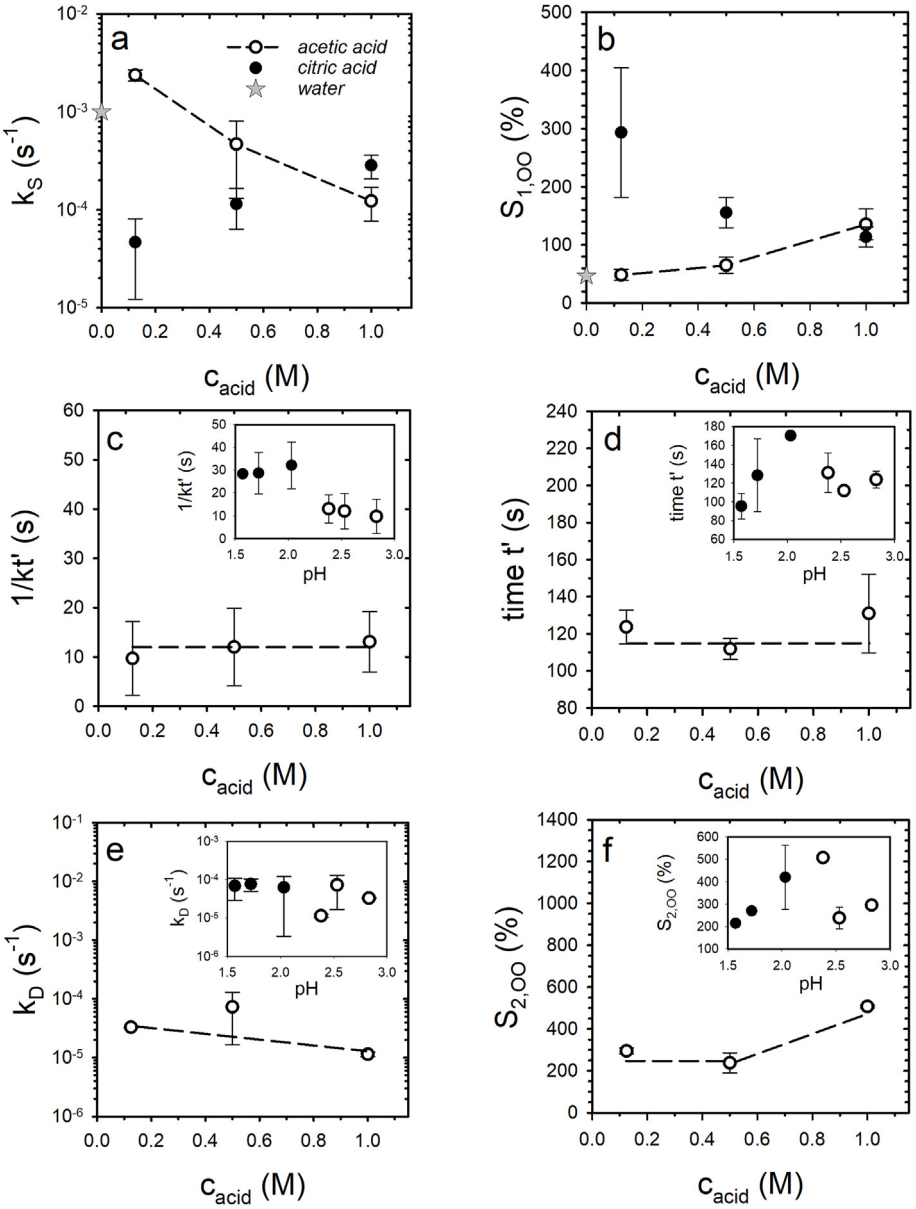

Fig. 4. Mean values of the model parameters (open symbols) used to simulate the swelling in acetic acid (Fig. 3). The connecting dashed lines indicate the trend. Parameter values for citric acid (Gebhardt & Darvishsefat, 2023) are shown as closed symbols for comparison or as a function of the pH of the acid in the inset. The values for swelling in water from Thill et al. (2022) are shown as asterisks as a comparison for the first swelling step.

0.125 M acetic acid (Fig. 3a). The thickness of the fiber swells very quickly within the first 10–20 s by 30–40% of its original thickness and keeps this value stable for about 100 s. This is followed by a very steep second swelling process, which is less pronounced in 0.5 and 1 M acetic acid. Instead of a plateau value at the end of the first swelling process, the fiber thicknesses continue to increase until the start of the second swelling process after approx. 120 s. In all acetic acid concentrations, no reliable swelling values could be measured after 200–220 s due to a lack of contrast. However, it is striking that at the end of the swelling kinetics, the smallest mean swelling values of the fiber were measured in 0.5 M acetic acid (Fig. 3b). Despite a much stronger curvature, all swelling curves could be described and analyzed in good approximation with the swelling model (Equation (4)) already successfully used for the swelling media hydrochloric acid and citric acid (Gebhardt & Darvishsefat, 2023; Thill et al., 2022). The values of the six model parameters were calculated by averaging the simulation results from the three independent swelling experiments and plotted as a function of the acid concentration in Fig. 4.

For 0.125 M acetic acid, the rate of the first swelling step k_S is of the same order of magnitude as that obtained for fiber swelling in pure water (Thill et al., 2022). With increasing acetic acid concentration, the swelling rate decreases and reaches a value in 1 M acetic acid that is approx. one order of magnitude smaller and was also observed for swelling in citric acid. In contrast to swelling in acetic acid, however, a slight increase in the swelling rate with increasing citric acid concentration was observed in earlier measurements (Gebhardt & Darvishsefat, 2023). The maximum values of the first swelling step $S_{1,\infty}$ also show an opposing trend for both organic swelling media. They increase in acetic acid with increasing acid concentration, while they decrease in citric acid before reaching similar values for both acids in 1-molar solution.

Based on the model parameters, it can be summarized that the first swelling step in 0.125 M acetic acid is very similar to swelling in water (Thill et al., 2022). In water, the fiber thickness swelled to a stable plateau value in a one-step process and remained stable. The hydration is driven by calcium chloride ions in the gel network originating from the coagulation bath of the fiber production. For the most dilute acetic acid (0.125 M), we also observe that the plateau value for the first swelling process remains stable for about 100 s (Fig. 3a). For 0.5 and 1 M acetic acid, however, the first plateau disappears due to the lower swelling rate k_s and the expansion continues instead (see Fig. 3b and c). In addition, there are large differences in the rate and maximum swelling value between acetic acid and citric acid at 0.125 M. Citric acid removes released calcium ions by chelation and thus destabilizes indirect calcium phosphate contacts between the caseins (Broyard & Gaucheron, 2015). This greatly reduces the swelling rate on the one hand and destabilizes the gel network on the other. At higher concentrations of the acids, the values for rate and plateau of the first swelling step become increasingly similar. However, since the pH values of both 1 M acids (pH 1.6 for 1 M citric acid and pH 2.37 for 1 M acetic acid) are very different, it can be concluded that the pH value of the medium does not play a crucial role in the initial phase of swelling.

During swelling, a transition area occurs towards a second swelling step. The swelling model describes this by two ratio functions, which are calculated using an exponential function and the associated rate kt' and characteristic time t'. The values for both parameters (see Fig. 4c and d) show no significant dependence on the acetic acid concentration and fluctuate around mean values of $kt' = 0.1\ s^{-1}$ (the reciprocal value is shown) and $t' = 127$ s.

The calculated ratio curves w_1 and w_2 add up to 1 and are mirror-symmetrical to the time-axis at value 0.5. The w_2 curves for acetic acid shown in Fig. 5 start after 50 s and extend over a period of approx. 100 s without a concentration-dependent trend. They differ greatly from the transition curves obtained for swelling in citric acid (Gebhardt & Darvishsefat, 2023), which are shown as dashed lines for comparison. These extend over a broader time range of 300 s due to lower rates (see insert Fig. 4c). Furthermore, they shift to shorter times with increasing citric acid concentration because of the concentration-dependent trend of the characteristic transition times (Fig. 4d).

For swelling step 2, the model analysis for the calculated plateau value $S_{2,\infty}$ shows a minimum for swelling in 0.5 M acetic acid. As already mentioned, this effect can also be seen in the measured swelling value at = 200 s (Fig. 3b) in comparison to the swellings in 0.125 M (Fig. 3a) and 1 M acetic acid (Fig. 3c). Due to the steeper transition curves compared to citric acid, swelling step 2 in acetic acid can be better observed and analyzed. A lower rate for swelling step 2 in 1 M acetic acid can be seen in the direct comparison of the measured data with 0.125 M acetic acid from the swelling curves and is confirmed by the model analysis via the corresponding values for k_D (Fig. 4e). It can be assumed that the pH value of the acids used has a significant influence on fiber swelling after the end of the second swelling step. The model parameters for the second swelling step and the transition are therefore shown with comparative values for citric acid (Gebhardt & Darvishsefat, 2023) as a function of the pH value of the acid solutions in the inserts of Fig. 4c–f. The pH range for acetic acid (pH 2.3–3) follows that for the stronger citric acid (pH 1.5–2.2). Compared to swelling in citric acid, a significant reduction in the rate of the second swelling process with pH can only be observed for the 1 M acids. Regardless of the acid, there is a weak trend towards lower rates with increasing pH value of the acids used. While a scaling behavior for the maximum expansion for the second swelling step as a function of pH was observed in citric acid and 1 M acetic acid (Gebhardt & Darvishsefat, 2023), the simulated final value shows a drastic reduction for $S_{2,\infty}$ at pH 2.3 and higher, i.e. for the swellings in 0.5 M and 0.125 M acetic acid.

Based on the model analysis, the swelling of two different parts of the fiber structure can be considered separately. For this purpose, the product of the swelling rate of the assigned swelling step and the corresponding proportion is integrated according to Equation (7). Fig. 6 shows how the proportions of both swollen casein structures change over time for all three acetic acid concentrations. The first swelling process (filled area) belongs to swelling step 1 and can be assigned to the hydration of the dry fiber and the dissociation of calcium bound on casein. The curve with the shaded

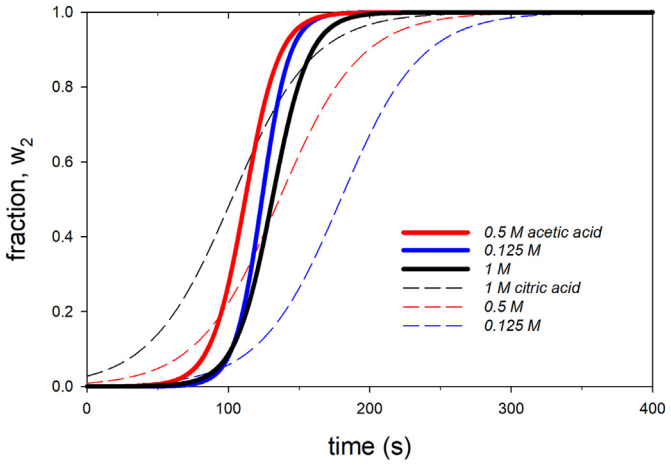

Fig. 5. Calculated ratio curves w_2 for swelling in 0.125 M (blue), 0.5 M (red) and 1 M acetic acid (black). Corresponding functions for citric acid from Gebhardt and Darvishsefat (2023) are shown as dashed lines for comparison.

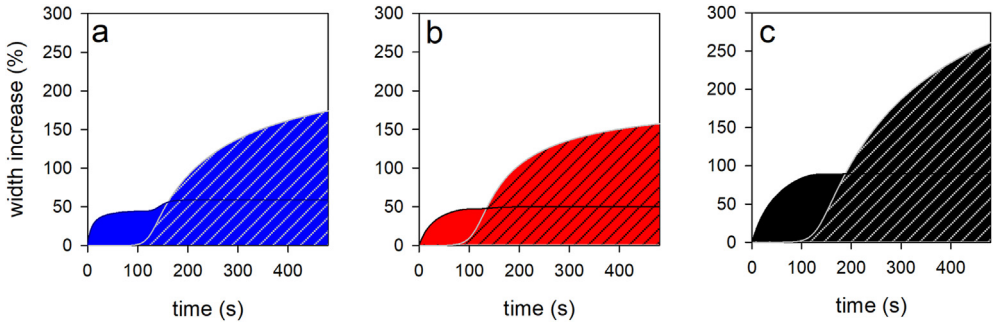

Fig. 6. Variation of the swollen rennet gel (filled area) and the swollen acidified rennet gel (shaded area) as a function of time in a) 0.125 M, b) 0.5 M and c) 1 M acetic acid.

area, on the other hand, corresponds to a swollen fiber structure that forms when the colloidal calcium phosphate has completely dissolved. Initially, within the first 100 s in 0.125 and 0.5 M acetic acid, there is an increase in fiber thickness to a plateau value of approx. 50%, which was also observed for pure water swelling at pH 7. However, the results also show a reduction in the swelling rate and an increase in the plateau value with increasing acetic acid concentration. These effects can therefore be attributed to the faster acidification of the fiber. As a result, the negative charge state of the caseins is reduced more quickly, whereby the electrostatic repulsion decreases. This could result in a denser rennet gel structure of the fiber in the early phase and a reduced swelling rate. During the initial swelling process, however, higher acetic acid concentrations could also weaken the gel structure by dissolving calcium contacts, which would explain higher plateau values or $S_{1,\infty}$ values. From approx. 100 s further swelling of the casein structure (shaded area) occurs as a result of the second swelling step. The sigmoidal increase is typical for gel formation processes and has been observed in rheological studies, e.g. for the course of the storage modulus during acid- or rennet-induced milk gel formation (Horne, 1999; Zoon, 1988). More precisely, the S-shaped curve of the model simulation is the result of the weighting of swelling step 2 with the ratio curve w_2 and thus describes the transition to an acidified rennet gel without colloidal calcium phosphate. The associated increase in fiber thickness can be attributed to the accumulation of water on caseins around their phosphoseryl-clusters. These bind colloidal calcium phosphate (Hindmarsh & Watkinson, 2017), which completely decomposes during acidification (Gaucheron, 2005). Differences due to different acidification rates between 0.125 M and 1 M acetic acid cannot be detected based on the results of the analysis (see ratio curves in Fig. 5). In contrast to swelling in citrate, however, dissociation takes place in a narrower time range. Citrate as a calcium chelator also destabilizes colloidal calcium phosphate in the neutral pH range, which initiates the second swelling process at an earlier phase and results in broader transition curves. In detail, citrate chelates ionic calcium in the aqueous phase and reduces the degree of saturation of the calcium phosphate there, resulting in solubilization of the micellar calcium phosphate (Broyard & Gaucheron, 2015). The increase in fiber thickness in the second swelling step can thus be attributed to the hydration of the phosphoseryl-cluster regions in an acidic rennet gel, as stabilizing calcium phosphate contacts no longer exist.

4. Conclusion

A two-step swelling mechanism in acetic acid was observed for fibers produced by extrusion of cold-stored casein micelles into a warm, calcium-rich coagulation bath. In 0.125 M acetic acid, both swelling steps are clearly separated from each other. However, in 0.5 and 1 M acetic acid, the swelling steps merge into each other, which was also observed at higher citric acid concentrations. We attribute this to the loss of micellar bound calcium, which is stronger in more acidic media and is further enhanced by a calcium chelator such as citrate. The first expansion step corresponds to the swelling of a rennet casein gel, while the second step can be assigned to the swelling of an acidified rennet gel. A sequential 6-parameter model describes not only the complex swelling kinetics in HCl and citric acid, but, as this study shows, also in acetic acid. While in 1 M HCl a clearly different behavior occurs due to deswelling to a stable final swelling value, the two-stage fiber expansion in acetic acid and in citric acid can be analyzed comparatively. We observe clear differences in the steepness of the transition between the two gel types during acidification and in the final values of both swelling steps. While the two swelling steps are clearly separated in acetic acid, they merge more strongly in citric acid. This is because citric acid, as a chelating agent, demineralizes the casein gel already at the beginning of the swelling process. It can also be observed that, in contrast to citric acid, the plateau values of both swelling stages increase with increasing acetic acid concentration. At the beginning of swelling, a higher concentration of acetic acid causes a larger number of dissociated ions within the gel network. This increases the swelling and leads to higher plateau values of the first swelling step. During the second swelling step, the pH values are below the isoelectric point of the caseins, and all calcium and inorganic phosphates of the fiber are completely dissolved. The increased swelling values can rather be explained by the increased electrostatic repulsion within the acidified rennet gel due to protonation, which occurs more strongly at higher acetic acid concentrations.

No evidence of fiber disintegration was observed in this study that would question the assumed stable plateau values of the swelling model. To investigate this aspect in more detail, future studies should employ high-resolution microscopic studies using fluorescent dyes to investigate the integrity of the fiber, especially at the end of the swelling process.

CRediT authorship contribution statement

Novin Darvishsefat: Writing – review & editing, Visualization, Validation, Methodology, Investigation, Conceptualization. **Md Asaduzzaman:** Writing – review & editing, Validation, Investigation. **Calvin Hohn:** Writing – review & editing, Validation, Investigation. **Ronald Gebhardt:** Writing – review & editing, Writing – original draft, Visualization, Validation, Supervision, Resources, Project administration, Methodology, Formal analysis, Conceptualization.

Declaration of competing interest

The authors declare that they have no known competing financial interests or personal relationships that could have appeared to influence the work reported in this paper.

Acknowledgements

The authors thank Sebastian Thill for helpful discussions.

References

Asaduzzaman, M., Pütz, T., & Gebhardt, R. (2022). Citrate effect on the swelling behaviour and stability of casein microparticles. *Scientific Reports, 12*(1), Article 18401.

Bar-Zeev, M., Kelmansky, D., Assaraf, Y. G., & Livney, Y. D. (2018). β-Casein micelles for oral delivery of SN-38 and elacridar to overcome BCRP-mediated multidrug resistance in gastric cancer. *European Journal of Pharmaceutics and Biopharmaceutics, 133*, 240–249.

Broyard, C., & Gaucheron, F. (2015). Modifications of structures and functions of caseins: A scientific and technological challenge. *Dairy Science & Technology, 95*, 831–862.

Chen, L., Wei, J., An, M., Zhang, L., Lin, S., Shu, G., et al. (2020). Casein nanoparticles as oral delivery carriers of mequindox for the improved bioavailability. *Colloids and Surfaces B: Biointerfaces, 195*, Article 111221.

Dalgleish, D. G. (2011). On the structural models of bovine casein micelles—review and possible improvements. *Soft Matter, 7*(6), 2265–2272.

Dalgleish, D. G., & Corredig, M. (2012). The structure of the casein micelle of milk and its changes during processing. *Annual Review of Food Science and Technology, 3*, 449–467.

Dalgleish, D. G., & Law, A. J. (1988). pH-induced dissociation of bovine casein micelles. I. Analysis of liberated caseins. *Journal of Dairy Research, 55*(4), 529–538.

De Kruif, C. G., & Zhulina, E. B. (1996). κ-casein as a polyelectrolyte brush on the surface of casein micelles. *Colloids and Surfaces A: Physicochemical and Engineering Aspects, 117*(1–2), 151–159.

Dumpler, J., Kieferle, I., Wohlschläger, H., & Kulozik, U. (2017). Milk ultrafiltrate analysis by ion chromatography and calcium activity for SMUF preparation for different scientific purposes and prediction of its supersaturation. *International Dairy Journal, 68*, 60–69.

Gastaldi, E., Trial, N., Guillaume, C., Bourret, E., Gontard, N., & Cuq, J. L. (2003). Effect of controlled κ-casein hydrolysis on rheological properties of acid milk gels. *Journal of Dairy Science, 86*(3), 704–711.

Gaucheron, F. (2005). The minerals of milk. *Reproduction Nutrition Development, 45*(4), 473–483.

Gebhardt, R., & Darvishsefat, N. (2023). Regenerated fibers from rennet-treated casein micelles during acidification. *Gels, 9*(7), 538.

Heidebach, T., Först, P., & Kulozik, U. (2009). Microencapsulation of probiotic cells by means of rennet-gelation of milk proteins. *Food Hydrocolloids, 23*(7), 1670–1677.

Hindmarsh, J. P., & Watkinson, P. (2017). Experimental evidence for previously unclassified calcium phosphate structures in the casein micelle. *Journal of Dairy Science, 100*(9), 6938–6948.

Horne, D. S. (1999). Formation and structure of acidified milk gels. *International Dairy Journal, 9*(3–6), 261–268.

Horne, D. S., & Lucey, J. A. (2017). Rennet-induced coagulation of milk. In *Cheese* (pp. 115–143). Academic Press.

Metzger, L. E., Barbano, D. M., Rudan, M. A., & Kindstedt, P. S. (2000). Effect of milk preacidification on low fat Mozzarella cheese. I. Composition and yield. *Journal of Dairy Science, 83*(4), 648–658.

Sadiq, U., Gill, H., & Chandrapala, J. (2021). Casein micelles as an emerging delivery system for bioactive food components. *Foods, 10*(8), 1965.

Schott, H. (1992). Swelling kinetics of polymers. *Journal of Macromolecular Science, Part B: Physics, 31*(1), 1–9.

Seth, K., & Bajwa, U. (2015). Effect of acidulants on the recovery of milk constituents and quality of Mozzarella processed cheese. *Journal of Food Science and Technology, 52*, 1561–1569.

Sudha, T. B., Thanikaivelan, P., Ashokkumar, M., & Chandrasekaran, B. (2011). Structural and thermal investigations of biomimetically grown casein–soy hybrid protein fibers. *Applied Biochemistry and Biotechnology, 163*, 247–257.

Thill, S., & Gebhardt, R. (2022). Effect of glycerol, calcium and transglutaminase post-treatment on the properties of regenerated fibers from rennet-treated casein micelles. *Colloids and Interfaces, 6*(2), 17.

Thill, S., Schmidt, T., Jana, S., Wöll, D., & Gebhardt, R. (2022). Fine structure and swelling properties of fibers from regenerated rennet-treated casein micelles. *Macromolecular Materials and Engineering, 307*(10), Article 2200272.

Thill, S., Schmidt, T., Wöll, D., & Gebhardt, R. (2020). Single particle tracking as a new tool to characterise the rennet coagulation process. *International Dairy Journal, 105*, Article 104659.

Thill, S., Schmidt, T., Wöll, D., & Gebhardt, R. (2021). A regenerated fiber from rennet-treated casein micelles. *Colloid and Polymer Science, 299*, 909–914.

Tomasula, P. M., Sousa, A. M., Liou, S. C., Li, R., Bonnaillie, L. M., & Liu, L. (2016). Electrospinning of casein/pullulan blends for food-grade applications. *Journal of Dairy Science, 99*(3), 1837–1845.

Warncke, M., Keienburg, S., & Kulozik, U. (2021). Cold-renneted milk powders for cheese production: Impact of casein/whey protein ratio and heat on the gelling behavior of reconstituted rennet gels and on the survival rate of integrated lactic acid bacteria. *Foods, 10*(7), 1606.

Yang, Y., & Reddy, N. (2012). Properties and potential medical applications of regenerated casein fibers crosslinked with citric acid. *International Journal of Biological Macromolecules, 51*(1–2), 37–44.

Zoon, P. (1988). *Rheological properties of rennet-induced skim milk gels*. PhD Thesis. The Netherlands: Wageningen Agricultural University.